

# Electron-phonon Coupling on the Surface of the Topological Insulator $\text{Bi}_2\text{Se}_3$ : Determined from Surface Phonon Dispersion Measurements

Xuetao Zhu<sup>1</sup>, L. Santos<sup>2</sup>, C. Howard<sup>1</sup>, R. Sankar<sup>3</sup>, F.C. Chou<sup>3</sup>, C. Chamon<sup>1</sup>, M. El-Batanouny<sup>1\*</sup>

<sup>1</sup>Department of Physics, Boston University, Boston, MA 02215, USA

<sup>2</sup>Department of Physics, Harvard University, Cambridge, MA 02138, USA

<sup>3</sup>Center of Condensed Matter Sciences, National Taiwan University, Taipei 10617, Taiwan

(Dated: February 6, 2012)

In this letter we report measurements of the coupling between Dirac fermion quasiparticles (DFQs) and phonons on the (001) surface of the strong topological insulator  $\text{Bi}_2\text{Se}_3$ . While most contemporary investigations of this coupling have involved examining the temperature dependence of the DFQ self-energy via angle-resolved photoemission spectroscopy (ARPES) measurements, we employ inelastic helium atom scattering to explore, for the first time, this coupling from the phonon perspective. Using a Hilbert transform, we are able to obtain the imaginary part of the phonon self-energy associated with a dispersive surface phonon branch identified in our previous work [1] as having strong interactions with the DFQs. From this imaginary part of the self-energy we obtain a branch-specific electron-phonon coupling constant of 0.43, which is stronger than the values reported from the ARPES measurements.

PACS numbers: 63.20.D-, 63.20.K-, 68.49.Bc, 72.10.Di

Topological insulators (TIs), a recently discovered class of materials with insulating bulk but exotic Dirac fermion metallic surface states [2–6], have become the focus of intense research by the condensed matter physics community. The strong spin-orbit coupling in TIs leads to a definite helicity whereby the spin is locked normal to the wavevector of the surface electronic state. A fundamental manifest feature of such spin-textured surface states is their robustness against spin-independent scattering, an attribute that protects them from backscattering and localization [7, 8]. In this sense, the surface states should be very stable in TIs. Indeed, ARPES and scanning tunneling microscopy (STM) have confirmed that the topological surface states are protected even against strong perturbations, provided they are spin-independent [9], even up to room temperature [10]. Consequently, electron-phonon (e-p) interaction should be the dominant scattering mechanism for surface Dirac fermions at finite temperatures. Hence, the study of e-p coupling in TIs is of exceptional importance in assessing potential applications such as spintronics.

In condensed matter physics the e-p interaction plays a dominant role in a myriad of phenomena ranging from electrical conductivity to superconductivity. As such, it has spawned an extensive amount of literature. E-p interaction changes the dispersion and the lifetime of both the electronic and phonon states in a material. The effect of the e-p coupling on the dispersion and lifetime of the states is contained in the complex self-energy  $\Sigma$  (electron) and  $\Pi$  (phonon). The real part  $\Sigma'$  ( $\Pi'$ ) renormalizes the dispersion, while the imaginary part  $\Sigma''$  ( $\Pi''$ ) accounts for the finite lifetime  $\tau$  of the state arising from the interaction. In spectroscopic terms, the linewidth (full width at half maximum)

$$\Gamma = \frac{\hbar}{\tau} = -2\Sigma''(\Pi''), \quad (1)$$

is frequently used. Because the real and imaginary parts of the self-energy are related by a Hilbert (or Kramers-Kronig)

transformation, it is sufficient to determine either  $\Sigma'$  ( $\Pi'$ ) or  $\Sigma''$  ( $\Pi''$ ). We should note that when determining the self-energy associated with an electronic state one integrates over all phonon states, and vice-versa. One can then study the e-p coupling and its consequences from the electron or phonon perspective. Here we report on our investigation of the e-p coupling from measurements of phonon dispersions. To the best of our knowledge this presents the first attempt at such an approach.

In this report we employ the dimensionless parameter  $\lambda$  to quantify the e-p coupling. It is defined by [11]

$$\lambda = 2 \int_0^{\omega_{max}} \frac{\alpha^2 F(\omega)}{\omega} d\omega, \quad (2)$$

where  $\alpha^2 F(\omega)$ , the so called Éliashberg e-p coupling function, is a product of an effective e-p coupling  $\alpha^2$  involving phonons of energy  $\hbar\omega$  and the phonon density of states  $F(\omega)$ . Previous attempts to quantify the e-p coupling from phonon measurements focused on extracting the e-p matrix element [12] rather than  $\lambda$ , a topic that we reported on in our previous paper [1].

Because of recent improvements in energy and momentum resolution of ARPES, it is now possible to obtain detailed information about the strength of e-p interaction as a function of the energy  $\epsilon_i$  and wavevector  $\mathbf{k}$  of electronic states. Yet, extracting such information on the e-p interaction from experimental data is not straightforward; it requires approximations that depend on the properties of the system studied. By measuring the electron's self-energy in the vicinity of the Fermi energy ( $E_F$ ) as a function of temperature, one can fit the ensuing temperature-dependence of lifetime broadening  $\Gamma_{e-p}(\epsilon_i, \mathbf{k})$  to the relation [11]

$$\Gamma_{e-p}(\epsilon_i, \mathbf{k}; T) = 2\pi\lambda(\epsilon_i, \mathbf{k}) k_B T, \quad (3)$$

valid at high temperatures, and extract the value of  $\lambda$ . Yet, using ARPES experiments to provide data capable of identifying

contributions of individual phonon modes to the e-p coupling remains elusive [13].

The strong three-dimensional TI  $\text{Bi}_2\text{Se}_3$ , which is the subject of this report, was found to have a single Dirac cone with a Dirac point at the SBZ center [14, 15]. Because of this simplicity, it has been extensively studied both experimentally and theoretically. ARPES studies have been recently extended to cover e-p coupling in  $\text{Bi}_2\text{Se}_3$  [16–18]. However, the results of the reported studies are contradictory. The ARPES measurements in Ref. 16 and Ref. 17, using Eq. (3), conclude that the e-p coupling in  $\text{Bi}_2\text{Se}_3$  is exceptionally weak, with a value of the dimensionless e-p coupling parameter  $\lambda \sim 0.08$  [17]. Yet, Ref. 18, using the same ARPES approach and Eq. (3), reports a much stronger coupling with  $\lambda \sim 0.25$ . All of the aforementioned studies are from the electron perspective, where the e-p interaction is integrated over all phonon modes. By contrast, effects of the e-p coupling on specific phonon modes are not commonly investigated.

From the phonon perspective, it is preferable to express the Éliashberg coupling function in terms of phonon mode linewidths and frequencies, and write the e-p coupling parameter  $\lambda$  as [19–21]

$$\begin{aligned}\lambda &= \frac{1}{2\pi N(E_F)} \frac{V_a}{(2\pi)^3} \int d^3q \sum_j \frac{\gamma_j(\mathbf{q}, \omega_{j\mathbf{q}})}{\hbar^2 \omega_{j\mathbf{q}}^2} \\ &= \frac{V_a}{(2\pi)^3} \int d^3q \sum_j \lambda_j(\mathbf{q}, \omega_{j\mathbf{q}}),\end{aligned}\quad (4)$$

where  $N(E_F)$  is the electronic density of states at  $E_F$ ,  $V_a$  is the primitive cell volume in real space,  $\gamma_j(\mathbf{q}, \omega_{j\mathbf{q}})$  is the linewidth of the  $j$ th mode at wavevector  $\mathbf{q}$  in eV,  $\omega_{j\mathbf{q}}$  is its frequency and  $\lambda_j(\mathbf{q}, \omega_{j\mathbf{q}})$  is the mode-specific e-p coupling.  $\lambda$  is then proportional to the sum of the  $\lambda_j(\mathbf{q}, \omega_{j\mathbf{q}})$  of the individual phonon branches averaged over the whole Brillouin zone.

Phonon line broadenings due to e-p coupling are generally small, even for superconductors with strong coupling. Such small broadenings are very difficult to detect in both neutron and helium scattering experiments mainly because of unavoidable instrument linewidths of a few meVs. This limits possibilities of extracting e-p broadening contributions from the measured phonon linewidth. Moreover, in addition to e-p coupling, there are other inherent contributions to phonon line broadening, such as phonon-phonon interaction (anharmonicity), phonon-defect scattering and phonon anti-crossing with other branches. Yet, if  $\Pi'$  can be determined, then it is straightforward to obtain  $\Pi''$  with the aid of a Hilbert transform.

Recently we reported experimental and theoretical results of surface phonon dispersions on  $\text{Bi}_2\text{Se}_3$  (001) [1]. The most prominent features are the absence of the acoustic Rayleigh branch, and the appearance of a low energy isotropic convexly dispersive surface optical phonon branch, here on denoted by  $\beta$ , with an energy maximum of 7.4 meV. It exhibited a V-shaped minimum at approximately  $2k_F$ , reflecting a strong Kohn anomaly. It is the lowest lying surface phonon branch

within  $2k_F$ . Our theoretical analysis attributed this dispersive profile to the renormalization of the surface phonon excitations by interactions with surface Dirac fermions. The contribution of the Dirac fermions to this renormalization was derived in terms of a Coulomb-type perturbation model within the random phase approximation (RPA), yielding an effective interaction strength [22] for the  $\beta$  branch of about 3.4 eV/Å [1]. In this letter, we show that because the energy renormalization of the  $\beta$  branch is mainly due to e-p coupling, we can simply use the Hilbert transform to obtain the e-p coupling parameter  $\lambda_\beta$  for this specific surface phonon branch  $\beta$ .

We carried out inelastic helium atom surface scattering (HASS) measurements for *in situ* cleaved (001) surface of  $\text{Bi}_2\text{Se}_3$ , at different temperatures in the range 80 K - 300 K. In Fig. 1 we show the experimental data for 300 K and 100 K (red and blue dots, respectively) for the  $\beta$  branch along the  $\bar{\Gamma}$ - $\bar{M}$  direction, as well as theoretical fits obtained with the pseudo-charge model and RPA [1]. Although on average the energy of the 100 K data points is slightly lower at a given wavevector  $q$  than those at 300 K, the difference is certainly quite small, which justifies carrying out the theoretical calculations at  $T = 0$  K. A very good agreement between theory and experiment is clearly seen.

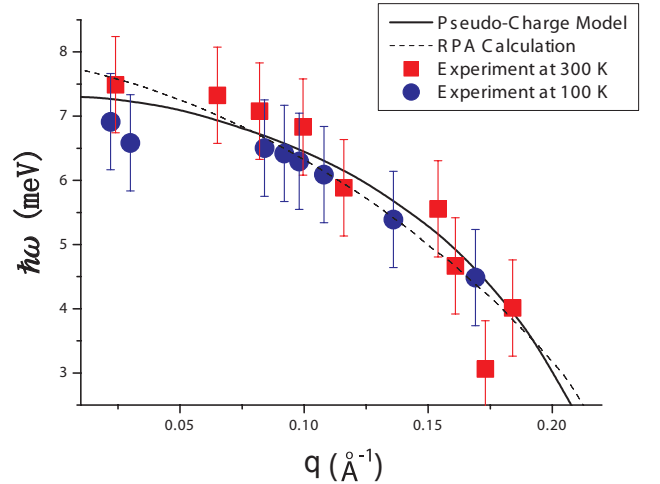


FIG. 1. Dispersion curve of the isotropic phonon branch  $\beta$ . The red squares represent the experimental data collected at 300 K, while the blue circles represent the data collected at 100 K. Vertical error bars indicate the energy resolution of our facility. The solid line is the result of the computational implementation of the pseudo-charge model. The dashed line represents the theoretical RPA calculation of the renormalized phonon energy [1].

Such measurements were also performed on two different samples at fixed incident and scattered angles, while varying the temperature. Fig. 2 (a) shows the temperature dependence of a phonon mode of the  $\beta$  branch at  $q \sim 0.13 \text{ Å}^{-1}$ . The phonon energy exhibits a very small increase with temperature, which is consistent with the trend shown in Fig. 1. Fig. 2 (b) shows the temperature dependence of a phonon mode

outside the  $\beta$  branch at  $q \sim 0.6 \text{ \AA}^{-1}$ . Consequently, a linear fit to the data has a very small slope, which justifies neglecting the temperature dependence, in particular, when we take into account an instrument resolution of about 1.5 meV. These results demonstrate that contributions from anharmonicity and defects can be ignored. It also justifies considering only e-p interaction in our theoretical RPA calculations.

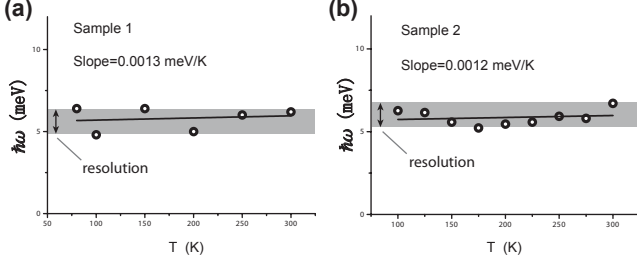


FIG. 2. The energy of a single phonon event as a function of temperature for Sample 1 at  $q \sim 0.13 \text{ \AA}^{-1}$  (a) and for Sample 2 at  $q \sim 0.6 \text{ \AA}^{-1}$  (b), respectively. The circles represent the experimental data, while the solid line stands for a linear fit of the data. The gray band represents the energy resolution of our facility.

Renormalization of phonon frequencies due to the e-p coupling is described by the Dyson equation

$$(\hbar\omega_{\mathbf{q},\beta})^2 = (\hbar\omega_{\mathbf{q},\beta}^{(0)})^2 + 2(\hbar\omega_{\mathbf{q},\beta}^{(0)}) \text{Re} [\Pi(\mathbf{q}, \omega_{\mathbf{q},\beta})], \quad (5)$$

where  $\omega_{\mathbf{q},\beta}$  and  $\omega_{\mathbf{q},\beta}^{(0)}$  are the renormalized and bare surface phonon frequency for the  $\beta$  branch, respectively, and  $\Pi(\mathbf{q}, \omega_{\mathbf{q},\beta})$  is the corresponding phonon self-energy. An explicit expression for  $\Pi(\mathbf{q}, \omega_{\mathbf{q},\beta})$  is given in Ref. 1 [23]. We used the best-fit parameters obtained in Ref. 1 to calculate  $\Pi'(\mathbf{q}, \omega_{\mathbf{q},\beta})$  for the  $\beta$  branch at different wavevectors along the  $\bar{\Gamma}$ - $\bar{M}$  direction. We obtain the corresponding  $\Pi''(\mathbf{q}, \omega_{\mathbf{q},\beta})$  using the Hilbert transform

$$\Pi''(\mathbf{q}, \omega_{\mathbf{q},\beta}) = \frac{2}{\pi} \int_0^\infty \frac{\omega_{\mathbf{q},\beta}}{\omega_{\mathbf{q},\beta}^2 - \omega'^2_{\mathbf{q},\beta}} \Pi'(\mathbf{q}, \omega'_{\mathbf{q},\beta}) d\omega'_{\mathbf{q},\beta}. \quad (6)$$

We plot the results for  $\Pi'$  and  $\Pi''$  in panels (a) and (b) of Fig. 3 respectively.

The phonon linewidth (FWHM) for the  $\beta$  branch, defined as [11]

$$\gamma_\beta(\mathbf{q}) = -2\Pi''(\mathbf{q}, \omega_{\mathbf{q},\beta}), \quad (7)$$

is plotted in Fig. 3 (c) as a function of the wavevector  $q$  along the  $\bar{\Gamma}$ - $\bar{M}$  direction. We note that the shape of  $\gamma_\beta(\mathbf{q})$  reflects the density of the final states for DFQ scattering. Moreover, the asymmetry apparent in the steep drop as  $q$  approaches  $2k_F \sim 0.2 \text{ \AA}^{-1}$  stems from the suppression of DFQ scattering events connecting states with progressively opposing spins at the far sides of the circular Fermi surface, as shown in Fig. 4.

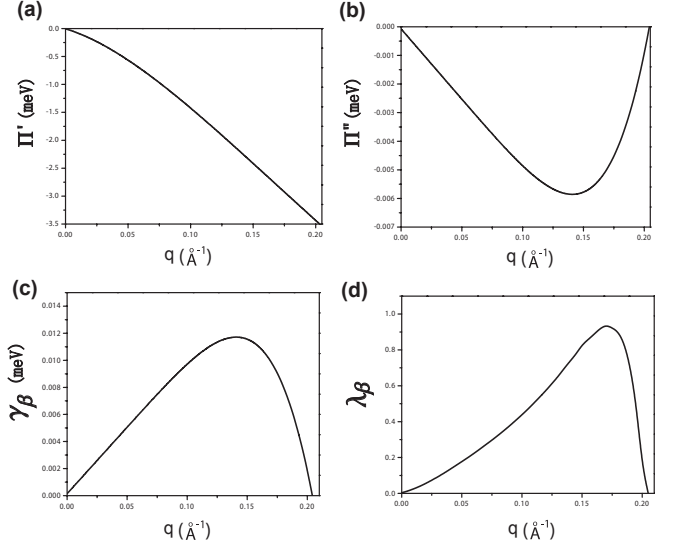


FIG. 3. (a) The real part of the self-energy  $\Pi'$ , and (b) its Hilbert transform  $\Pi''$ , for the isotropic phonon branch  $\beta$ . (c) The linewidth  $\gamma_\beta = -2\Pi''$ , and (d) the coupling parameter  $\lambda_\beta(q)$  determined from  $\gamma_\beta$ .

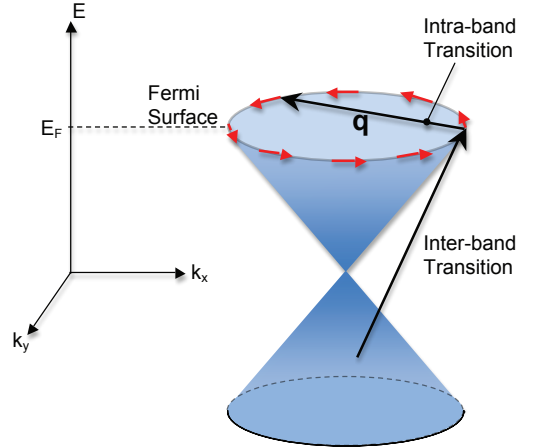


FIG. 4. Intra- and Inter-band transitions of DFQs that contribute to the renormalization of the prominent surface phonon branch  $\beta$ .  $\mathbf{q}$  is the phonon wave vector. The red arrows indicate the spin helicity on the Fermi Surface.

We obtain the corresponding e-p coupling  $\lambda_\beta(q)$ , shown in Fig. 3 (d), with the aid of the expression

$$\lambda_\beta(\mathbf{q}) = \frac{1}{2\pi N(E_F)} \frac{\gamma_\beta(\mathbf{q})}{\hbar^2 \omega_{\mathbf{q},\beta}^2}, \quad (8)$$

as derived from Eq. (4). Averaging over the function  $\lambda_\beta(q)$ , we obtain an effective e-p coupling constant value for the  $\beta$  branch  $\lambda_\beta = 0.43$ , which is greater than the reported values of 0.25 [18] and 0.08 [17] obtained from the ARPES measurements. This value of  $\lambda_\beta$ , extracted from our experimen-

tal data, presents a lower bound on the actual value of the overall e-p coupling constant  $\lambda$ . However, additional contributions from the remaining higher surface phonon branches to  $\lambda$  are not expected to increase its value significantly above  $\lambda_\beta$ . The reason is that the dispersions of each of these higher branches appear the same regardless of the presence or absence of the DFQs as evidenced from our lattice dynamics calculations based on the pseudo-charge model shown in figures 2 and 3 in Ref. [1]. Moreover, our result is supported by a recent optical infrared study [24], which suggests a strong e-p coupling for the  $61 \text{ cm}^{-1}$  (or  $7.6 \text{ meV}$ ) optical phonon mode. Also, a recent theoretical study based on an isotropic elastic continuum phonon model, where e-p coupling involves an acoustic phonon branch, obtains a value of  $\lambda \sim 0.42$  for thin film geometry [25], and  $\lambda \sim 0.84$  for semi-infinite geometry [26] of  $\text{Bi}_2\text{Se}_3$ . We note, however, that our experimental data demonstrates the absence of acoustic surface phonon modes [1].

In summary we use inelastic HASS measurements to determine the e-p coupling constant for a specific surface phonon branch of  $\text{Bi}_2\text{Se}_3$ . Direct experimental measurement of the e-p contribution to the phonon linewidth is difficult, so instead we obtain it by extracting the real part of the phonon self-energy using an RPA fit to the measured surface phonon dispersion curve, and then obtaining the imaginary part, and hence the e-p contribution to the phonon linewidth, with the aid of a Hilbert transform. This approach is supported by the fact that the experimentally measured temperature independence of the dispersion demonstrates that the surface phonon frequency renormalization is mainly determined by e-p coupling. Using this procedure we find an average e-p coupling parameter for the specific phonon branch  $\lambda_\beta = 0.43$  that is greater than the values obtained from the ARPES measurements.

This work is supported by the U.S. Department of Energy under Grants No. DE-FG02-85ER45222 (MEB) and DEFG02-06ER46316 (CC). FCC acknowledges the support from the National Science Council of Taiwan under project No. NSC 99-2119-M-002-011-MY.

- 
- [1] X. Zhu, L. Santos, R. Sankar, S. Chikara, C. . Howard, F. C. Chou, C. Chamon, and M. El-Batanouny, *Phys. Rev. Lett.* **107**, 186102 (2011).
  - [2] M. Z. Hasan and C. L. Kane, *Rev. Mod. Phys.* **82**, 3045 (2010).
  - [3] X.-L. Qi and S.-C. Zhang, *Rev. Mod. Phys.* **83**, 1057 (2011).
  - [4] J. E. Moore, *Nature* **464**, 194 (2010).
  - [5] L. Fu and C. L. Kane, *Phys. Rev. B* **76**, 045302 (2007).

- [6] M. Z. Hasan and J. E. Moore, *Annual Review of Condensed Matter Physics* **2**, 55 (2011).
- [7] P. Roushan, J. Seo, C. V. Parker, Y. S. Hor, D. Hsieh, D. Qian, A. Richardella, M. Z. Hasan, R. J. Cava, and A. Yazdani, *Nature* **460**, 1106 (2009).
- [8] T. Zhang, P. Cheng, X. Chen, J.-F. Jia, X. Ma, K. He, L. Wang, H. Zhang, X. Dai, Z. Fang, X. Xie, and Q.-K. Xue, *Phys. Rev. Lett.* **103**, 266803 (2009).
- [9] L. A. Wray, S.-Y. Xu, Y. Xia, D. Hsieh, A. V. Fedorov, Y. S. Hor, R. J. Cava, A. Bansil, H. Lin, and M. Z. Hasan, *Nature Physics* **7**, 32 (2011).
- [10] D. Hsieh, Y. Xia, D. Qian, L. Wray, J. H. Dil, F. Meier, J. Osterwalder, L. Patthey, J. G. Checkelsky, N. P. Ong, A. V. Fedorov, H. Lin, A. Bansil, D. Grauer, Y. S. Hor, R. J. Cava, and M. Z. Hasan, *Nature* **460**, 1101 (2009).
- [11] G. Grimvall, *The electron-phonon interaction in metals* (North-Holland Publishing Company, 1981).
- [12] H. Qin, J. Shi, Y. Cao, K. Wu, J. Zhang, E. W. Plummer, J. Wen, Z. J. Xu, G. D. Gu, and J. Guo, *Phys. Rev. Lett.* **105**, 256402 (2010).
- [13] P. Hofmann, I. Y. Sklyadneva, E. D. L. Rienks, and E. V. Chulkov, *New Journal of Physics* **11**, 125005 (2009).
- [14] Y. Xia, D. Qian, D. Hsieh, L. Wray, A. Pal, H. Lin, A. Bansil, D. Grauer, Y. S. Hor, R. J. Cava, and M. Z. Hasan, *Nat. Phys.* **5**, 398 (2009).
- [15] H. Zhang, C.-X. Liu, X.-L. Qi, X. Dai, Z. Fang, and S.-C. Zhang, *Nat. Phys.* **5**, 438 (2009).
- [16] S. R. Park, W. S. Jung, G. R. Han, Y. K. Kim, C. Kim, D. J. Song, Y. Y. Koh, S. Kimura, K. D. Lee, N. Hur, J. Y. Kim, B. K. Cho, J. H. Kim, Y. S. Kwon, J. H. Han, and C. Kim, *New Journal of Physics* **13**, 013008 (2011).
- [17] Z. . Pan, A. V. Fedorov, D. Gardner, Y. S. Lee, S. Chu, and T. Valla, ArXiv e-prints (2011), [arXiv:1109.3638 \[cond-mat.str-el\]](https://arxiv.org/abs/1109.3638).
- [18] R. C. Hatch, M. Bianchi, D. Guan, S. Bao, J. Mi, B. B. Iversen, L. Nilsson, L. Hornekær, and P. Hofmann, *Phys. Rev. B* **83**, 241303 (2011).
- [19] P. B. Allen, *Phys. Rev. B* **6**, 2577 (1972).
- [20] W. H. Butler, F. J. Pinski, and P. B. Allen, *Phys. Rev. B* **19**, 3708 (1979).
- [21] P. Allen, *Dynamical Properties of Solids*, edited by G. Horton and A. Maradudin, Vol. 3 (North-Holland Publishing Company, 1980).
- [22] In Ref. 1 we used the notation  $\lambda$  to indicate the effective interaction strength between phonons and DFQs in the Hamiltonian. This should not be confused with the present discussion of the e-p coupling parameter  $\lambda$ , which, despite the similarity in notation, is a different quantity.
- [23] In Ref. 1  $\Pi$  is defined as the the polarization function; it needs to be multiplied by the prefactor  $\frac{|g_{\mathbf{q},\beta}|^2}{\varepsilon(\mathbf{q},\omega_{\mathbf{q},\beta})}$  to become the self-energy that appears in Eq. (5).
- [24] A. D. LaForge, A. Frenzel, B. C. Pursley, T. Lin, X. Liu, J. Shi, and D. N. Basov, *Phys. Rev. B* **81**, 125120 (2010).
- [25] S. Giraud, A. Kundu, and R. Egger, ArXiv e-prints (2011), [arXiv:1111.4063 \[cond-mat.mes-hall\]](https://arxiv.org/abs/1111.4063).
- [26] S. Giraud and R. Egger, *Phys. Rev. B* **83**, 245322 (2011).